

Supplemental Materials & Methods

Native gel-shift analysis of RI·RNase complexes

Ribonuclease inhibitors and ribonucleases from endogenous species were incubated together in a 1:1.2 molar ratio at 25 °C for 20 min to allow for complex formation. A 10- μ L aliquot of protein solution was combined with 2 μ L of a 6 \times loading dye, and the resulting mixtures were loaded immediately onto a non-denaturing 12% w/v polyacrylamide gel (BioRad). Gels were run in the absence of SDS at 20–25 mA for ~3 h at 4 °C and stained with Coomassie Brilliant Blue G-250 dye (Sigma Chemical).

RI inhibition of endogenous ribonucleolytic activity

Ribonuclease inhibitors were diluted to 10 μ M in PBS, and diluted serially across a 96-well plate to yield a final range of 0.001 pM–1 μ M RI. A fluorogenic RNA substrate was added to each well (0.2 μ M of 6-FAM–dArU(dA)₂–6-TAMRA from IDT) [1], and baseline fluorescent readings were recorded. Ribonucleases were added to a final concentration of 50 pM (human, bovine, mouse, chicken) or 500 pM (anole), and the initial velocity of substrate cleavage was measured by following the increase in fluorescence over time. After 10 min, substrate cleavage was saturated by the addition of 5 μ M bovine RNase A. Values of k_{cat}/K_M were determined for each RI concentration as described previously [1], and these values were normalized to those in the absence of RI. Values represent the mean of at least three independent experiments.

Ribonuclease phylogenetic tree reconstruction

Ribonuclease protein sequence alignments were made using MUSCLE [2] with manual adjustments. A maximum-likelihood phylogenetic tree was generated in MEGA5.2 [3] using the Whelan and Goldman (WAG) [4] substitution model and 1000 bootstrap replicates. Non-uniformity of evolutionary rates was modeled using a discrete Gamma distribution [5], assuming for the presence of invariable sites. Bootstrap values >40 are reported.

References

- [1] Kelemen, B. R., Klink, T. A., Behlke, M. A., Eubanks, S. R., Leland, P. A. & Raines, R. T. (1999). Hypersensitive substrate for ribonucleases. *Nucleic Acids Res.* **27**, 3696-3701.
- [2] Edgar, R. C. (2004). MUSCLE: Multiple sequence alignment with high accuracy and high throughput. *Nucleic Acids Res.* **32**, 1792-7.
- [3] Tamura, K., Peterson, D., Peterson, N., Stecher, G., Nei, M. & Kumar, S. (2011). MEGA5: Molecular evolutionary genetics analysis using maximum likelihood, evolutionary distance, and maximum parsimony methods. *Mol. Biol. Evol.* **28**, 2731-9.
- [4] Whelan, S. & Goldman, N. (2001). A general empirical model of protein evolution derived from multiple protein families using a maximum-likelihood approach. *Mol. Biol. Evol.* **18**, 691-9.
- [5] Yang, Z. (1994). Maximum likelihood phylogenetic estimation from DNA sequences with variable rates over sites: Approximate methods. *J. Mol. Evol.* **39**, 306-14.
- [6] Lomax, J. E., Eller, C. H. & Raines, R. T. (2012). Rational design and evaluation of mammalian ribonuclease cytotoxins. *Methods Enzymol.* **502**, 273-90.
- [7] Lee, F. S., Shapiro, R. & Vallee, B. L. (1989). Tight-binding inhibition of angiogenin and ribonuclease A by placental ribonuclease inhibitor. *Biochemistry* **28**, 225-230.
- [8] Abel, R. L., Haigis, M. C., Park, C. & Raines, R. T. (2002). Fluorescence assay for the binding of ribonuclease A to the ribonuclease inhibitor protein. *Anal. Biochem.* **306**, 100-107.
- [9] Zhu, X. & Mitchell, J. C. (2011). KFC2: A knowledge-based hot spot prediction method based on interface solvation, atomic density, and plasticity features. *Proteins* **79**, 2671-83.

Table S1. Oligonucleotides used in the cloning of novel ribonuclease and ribonuclease inhibitor genes

Gene	Restriction Enzyme	Primer Sequence
Mouse RNase 1 (forward)	<i>Nco</i> I	ATTATCATATGAGGGAATCTGCACAG
Mouse RNase 1 (reverse)	<i>Xho</i> I	AACTCGAGCTACACAGTAGCATCAAAG
Chicken RNase A-1 (forward)	<i>Nde</i> I	ATATAATCATATGGTTCCAACCTACCAAGATTTTTTGC
Chicken RNase A-1 (reverse)	<i>Sal</i> I	TATAATATGTCGACTCATGGAAAGGTGCCATCCAG
Anole RNase 1 (forward)	<i>Nde</i> I	AATATAATCATATGAGGGAAAGCCGTCATGAC
Anole RNase 1 (reverse)	<i>Sal</i> I	TTATAATATGTCGACCTAAAGAGGAGCTTTGAAG
Zebrafish RNase 3/4 (forward)	<i>Nde</i> I	CTATATATACATATGCAGTCTTATAATGACTTCAAAC
Zebrafish RNase 3/4 (reverse)	<i>Zho</i> I	CTATATATACTCGAGTTAAGAATTGTTGGAACGTC
Mouse RI (forward)	<i>Nde</i> I	CATATG ATGAGTCTTGACATCCAGTGTGAG
Mouse RI (reverse)	<i>Sal</i> I	GTCGAC CTTCCCTGAGGATCATTTCCTGA
Chicken RI (forward)	<i>Nde</i> I	CATGGACCTTGACATCCAGTGTGAGGAG
Chicken RI (reverse)	<i>Sal</i> I	ATTATTATATGTCGACTCATGAAATGATCTTCACATCAGG
Anole RI (forward)	<i>Nde</i> I	CATGGATCTTGACATCCAGTCTACCGAG
Anole RI (reverse)	<i>Sal</i> I	AATTATAATATGTCGACTCATGTAACCAATTTAAATCCAG

Table S2. Dissociation rate constants and equilibrium dissociation constants for intra- and inter-species RI·RNase complexes

		Human RI (<i>H. sapiens</i>)	Mouse RI (<i>M. musculus</i>)	Bovine RI (<i>B. taurus</i>)	Chicken RI (<i>G. gallus</i>)	Lizard RI (<i>A. carolinensis</i>)
Human RNase 1 (<i>H. sapiens</i>)	k_d (s ⁻¹) ^a	$(1.2 \pm 0.5) \times 10^{-8}$	$(5.4 \pm 3.2) \times 10^{-8}$	$(4.1 \pm 1.4) \times 10^{-8}$	$(1.2 \pm 0.7) \times 10^{-8}$	$(2.3 \pm 0.2) \times 10^{-8}$
	K_d (M) ^b	$(3.5 \pm 1.4) \times 10^{-17}$	$(1.6 \pm 1.0) \times 10^{-16}$	$(1.2 \pm 1.0) \times 10^{-16}$		
Mouse RNase 1 (<i>M. musculus</i>)	k_d (s ⁻¹)	$(7.9 \pm 1.9) \times 10^{-7}$	$(6.5 \pm 4.4) \times 10^{-8}$	$(6.3 \pm 3.8) \times 10^{-7}$	$(1.3 \pm 0.9) \times 10^{-8}$	$(7.6 \pm 0.2) \times 10^{-7}$
	K_d (M)	$(2.3 \pm 1.9) \times 10^{-15}$	$(1.9 \pm 1.3) \times 10^{-16}$	$(1.8 \pm 1.1) \times 10^{-15}$		
Bovine RNase A (<i>B. taurus</i>)	k_d (s ⁻¹)	$(3.8 \pm 2.4) \times 10^{-7}$	$(5.9 \pm 1.6) \times 10^{-7}$	$(5.6 \pm 3.1) \times 10^{-8}$	$(1.9 \pm 1.2) \times 10^{-8}$	$(7.5 \pm 0.1) \times 10^{-7}$
	K_d (M)	$(1.2 \pm 1.1) \times 10^{-15}$	$(1.7 \pm 1.2) \times 10^{-15}$	$(1.7 \pm 1.2) \times 10^{-16}$		
Chicken RNase (<i>G. gallus</i>)	k_d (s ⁻¹)		$(7.3 \pm 1.9) \times 10^{-9}$	$(1.2 \pm 0.5) \times 10^{-8}$	$(3.4 \pm 1.3) \times 10^{-7}$	$(2.7 \pm 1.5) \times 10^{-6}$
	K_d (M) ^c	$(3.1 \pm 0.7) \times 10^{-10}$			$(1.0 \pm 0.8) \times 10^{-15}$	$(8.0 \pm 0.1) \times 10^{-15}$
Lizard RNase (<i>A. carolinensis</i>)	k_d (s ⁻¹)		$(2.2 \pm 1.0) \times 10^{-8}$	$(3.9 \pm 0.1) \times 10^{-8}$	$(9.0 \pm 0.8) \times 10^{-7}$	$(5.4 \pm 3.1) \times 10^{-7}$
	K_d (M)	$(1.6 \pm 0.4) \times 10^{-9}$			$(2.6 \pm 0.2) \times 10^{-15}$	$(1.6 \pm 1.1) \times 10^{-15}$
Frog RNase (<i>R. pipiens</i>)	K_d (M)	$>10^{-3}$	$>10^{-3}$	$>10^{-3}$	$>10^{-3}$	$>10^{-3}$
Fish RNase (<i>D. rerio</i>)	K_d (M)	$>10^{-3}$	$>10^{-3}$	$>10^{-3}$	$>10^{-3}$	$>10^{-3}$

^a For intra-species complexes and high-affinity inter-species complexes, values of k_d (\pm SE) were determined by monitoring the release of diethylfluorescein-labeled ribonuclease from a RI·ribonuclease complex over time and fitting the resulting data as described previously [6].

^b For intra-species complexes and high-affinity inter-species complexes, values of K_d (\pm SE) were determined with the equation $K_d = k_d/k_a$ and the k_a value for human RI and RNase A [7].

^c For low-affinity inter-species complexes, values of K_d (\pm SE) were determined directly by measuring the fluorescent quenching of diethylfluorescein-labeled ribonucleases upon incubation with increasing concentrations of RI, and fitting the data as described previously [8].

Table S3. Percent identity/similarity^a and crystal structure RMSD^b between ribonuclease inhibitor homologs

	Human RI		Mouse RI		Bovine RI		Chicken RI		Anole RI	
Human RI ^c			82	1.05	83	0.80	66	0.86	64	ND
Mouse RI	73	1.05			84	0.83	65	1.14	66	ND
Bovine RI	74	0.80	77	0.83			66	1.03	65	ND
Chicken RI	49	0.86	49	1.14	49	1.03			76	ND
Anole RI	46	ND	45	ND	46	ND	60	ND		

^a Gray shading denotes percent similarity of residues, as calculated by: G=A=V=L=I; F=Y=W; C=M; S=T; K=R=H; D=E=N=Q

^b Bold typeface denotes RMSD values calculated with the program PyMOL.

^c PDB 1z7x.

ND; not determined.

Table S4. Percent identity/similarity^a and crystal structure RMSD^b between ribonuclease homologs

	Human RNase		Mouse RNase		Bovine RNase		Chicken RNase		Anole RNase		Frog RNase		Fish RNase	
Human RNase ^c			77	0.29	77	0.36	43	0.85	46	ND	33	1.31	30	ND
Mouse RNase	68	0.29			77	0.38	46	0.83	52	ND	35	1.01	32	ND
Bovine RNase	68	0.36	70	0.38			43	0.82	49	ND	37	1.22	34	ND
Chicken RNase	28	0.85	32	0.83	29	0.82			46	ND	33	1.47	32	ND
Anole RNase	38	ND	40	ND	38	ND	32	ND			37	ND	30	ND
Frog RNase ^d	21	1.31	22	1.01	23	1.22	18	1.47	22	ND			42	ND
Fish RNase	19	ND	20	ND	20	ND	21	ND	19	ND	26	ND		

^a Gray shading denotes percent similarity of residues, as calculated by: G=A=V=L=I; F=Y=W; C=M; S=T; K=R=H; D=E=N=Q

^b Bold typeface denotes RMSD values calculated with the program PyMOL.

^c PDB 1z7x.

^d PDB 3phn.

ND; not determined.

Table S5. GenBank accession numbers for ribonuclease inhibitor and ribonuclease sequences

Ribonuclease Inhibitors		Ribonucleases	
Species	Accession Number	Species	Accession Number
<i>H. sapiens</i>	NP_976323	<i>H. sapiens</i>	CAG29314
<i>P. troglodytes</i>	NP_001009060	<i>M. musculus</i>	EDL20847
<i>G. gorilla</i>	XP_004050395	<i>B. taurus</i>	NP_001014408
<i>M. mulatta</i>	XP_001116618	<i>G. gallus</i>	ABD60081
<i>P. anubis</i>	XP_003909365	<i>A. carolinensis</i>	XP_003223861
<i>C. jacchus</i>	JAB44758	<i>D. rerio</i>	ABQ23785
<i>C. griseus</i>	EGW05529	<i>R. pipiens</i>	AAI54383.1
<i>M. musculus</i>	NP_001165571		
<i>R. norvegicus</i>	BAJ22804		
<i>A. melanoleuca</i>	XP_002929526		
<i>F. catus</i>	XP_003993862		
<i>C. simum</i>	XP_004441085		
<i>E. caballus</i>	XP_001488525		
<i>B. taurus</i>	NP_001030396		
<i>O. orca</i>	XP_004278153		
<i>G. gallus</i>	NP_001006473		
<i>A. platyrhynchos</i>	EOB05008		
<i>P. humilis</i>	XP_005522432		
<i>G. fortis</i>	XP_005419558		
<i>C. livia</i>	XP_005509116		
<i>M. undulatus</i>	XP_005149280		
<i>A. mississippiensis</i>	XP_006263475		
<i>O. hannah</i>	ETE73461		
<i>A. carolinensis</i>	XP_003214831		

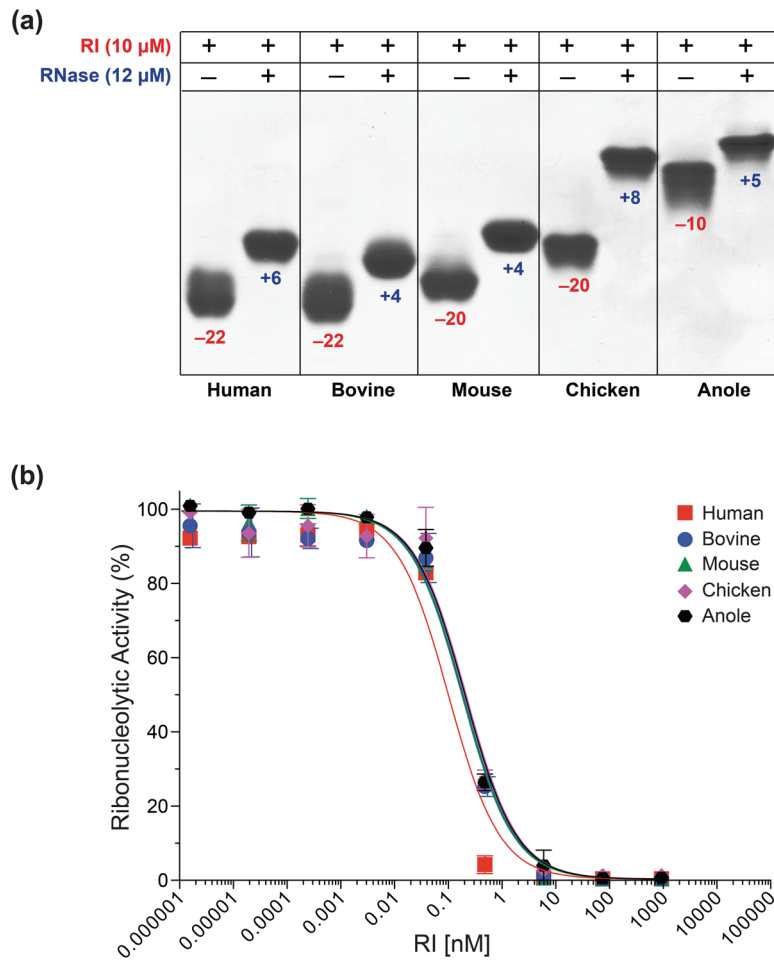


Fig. S1. Ribonuclease inhibitors bind and inhibit their cognate ribonucleases with 1:1 stoichiometry. (a) Native gel demonstrating the shift in the pI of RI induced by binding to its RNase. Values of Z for each RI (red) and cognate ribonuclease (red) are indicated for each species. (b) Ribonucleolytic activity of each RNase in panel A (human, bovine, mouse, chicken, 50 pM; anole, 500 pM) in the presence of increasing concentrations of its cognate RI.

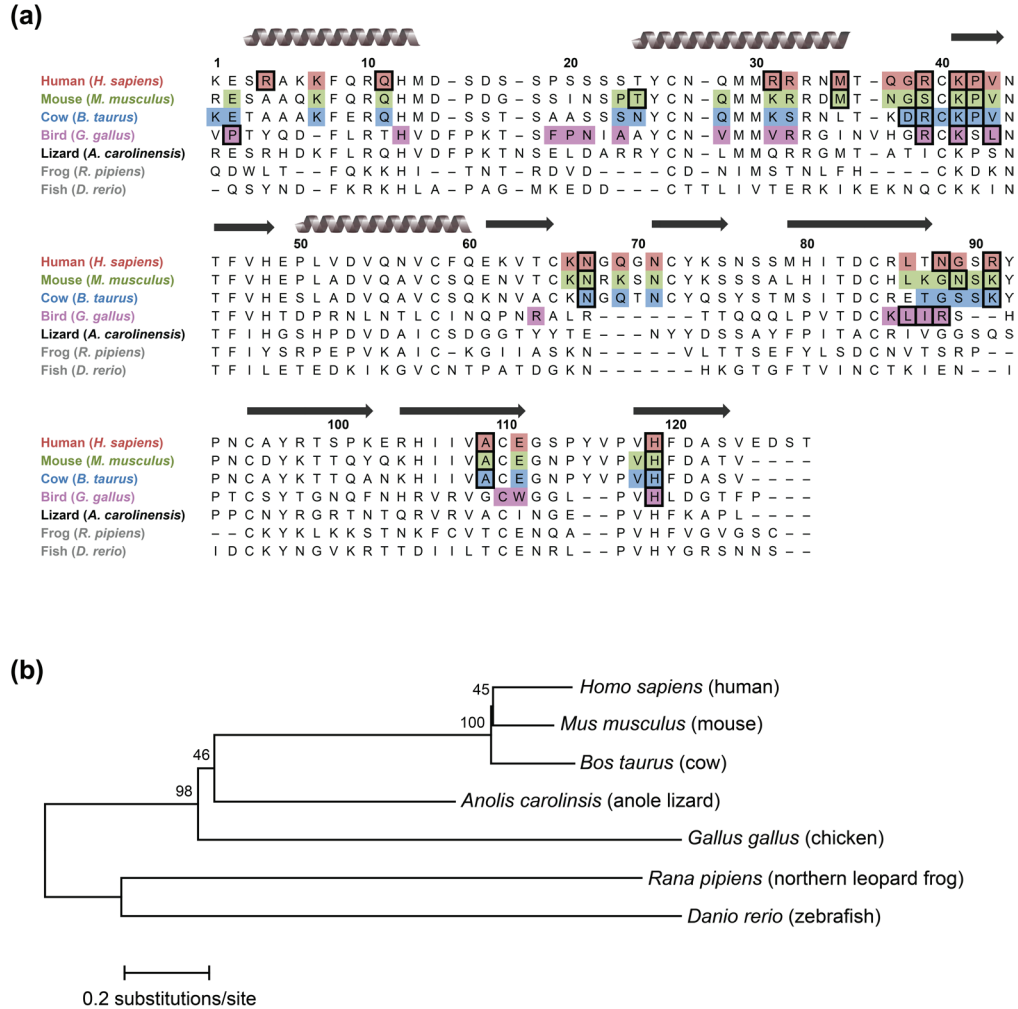


Fig. S2. Comparisons of homologous secretory ribonucleases. (a) Amino-acid sequence alignment showing endogenous RI-interface regions (shaded) based on analyses of crystal structures. Black boxes indicate predicted “hotspots” for binding affinity [9]. Gray coils represent α -helices; black arrows represent β -sheets. (b) Maximum-likelihood phylogenetic tree showing evolutionary relationships. Bootstrap values >40 are shown.